Modified Spontaneous Emission and Qubit Entanglement from Dipole-Coupled Quantum Dots in a Photonic Crystal Nanocavity

S. Hughes*

NTT Basic Research Laboratories, NTT Corporation, 3-1 Morinosato-Wakamiya, Atsugi, Kanagawa 243-0198, Japan

(Received 11 November 2004; revised manuscript received 7 February 2005; published 8 June 2005)

The modified spontaneous emission dynamics of two photon-coupled quantum dots in a planar-photonic crystal are theoretically investigated. Based on a photon Green function technique for quantizing the electromagnetic fields in arbitrary surroundings, pronounced vacuum Rabi oscillations and dipole-dipole interactions are self-consistently incorporated and are shown to result in a high degree of quantum-bit entanglement. Quantum dots with different optical dipole moments are also found to yield a very rich display of quantum dynamics and offer several advantages over coupling identical atoms.

DOI: 10.1103/PhysRevLett.94.227402 PACS numbers: 78.67.Hc, 41.20.Jb, 42.55.Tv, 42.70.Qs

Photonic crystals (PCs) have long promised a material environment that can change the spontaneous emission (SE) dynamics of excited atoms [1,2]. Recently, modified SE has been experimentally observed for quantum dots (QDs) imbedded in PCs, demonstrated for both broadband weak coupling and narrow band strong coupling regimes, in inverse opal structures [3] and semiconductor PC nanocavities [4], respectively. This latter phenomena introduces a new and hitherto unexplored regime in solid-state optics, namely, single QD strong coupling [5], and was partly motivated through tremendous progress with planar-photonic-crystal (PPC) nanocavities [6]. Here we suggest a possible way to realize exciton entanglement by dipole coupling the emission dynamics from two single photon emitters within a controlled photon environment that can be achieved through dipole-dipole-coupled QDs in PPC nanocavities. While a conceptually similar system has been used to generate entangled states in atoms within a superconducting cavity [7], the semiconductor problem requires much greater care in its description and the ensuing quantum dynamics is found to be much richer, especially for different QDs. In addition, the semiconductor system (QDs plus PPC nanocavity) offers many advantages over the atomic system, including the small size, integrability with waveguides, QDs that are fixed in position, large optical dipole moments, and transition energies (somewhat tunable) that are compatible with telecom applications. Envisioned applications range from scalable solid-state secure communication systems to novel photon switches.

The subject of two-path photon interference from a quantum optics perspective remains an intriguing fundamental optical regime that covers many branches of optical science, ranging from Young's famous double-slit experiment [8] to cavity coupling between two atoms [7]. Additionally, as semiconductor nanomaterials continue to achieve significant spatial confinement of both photons and electron-hole pairs, it is now possible to achieve enhanced emission and strong coupling effects of single QDs placed in PPC nanocavities [9]. Moreover, such coupling schemes may offer an efficient way to produce single photons and entangled photons, on demand, by exploiting the large Q (quality factor) and small mode volumes.

While exciting experimental observations are now coming to the fore, understanding the underlying physics that determine the optical coupling of semiconductor QDs within complex PCs remains a formidable challenge—a challenge that is too often attempted using brute force numerical techniques that offer little physical insight. To address these issues, and to tackle our desired coupled QD system, in this Letter we describe and apply a photon Green function tensor (GFT) technique to study the influence of cavity and dipole coupling on the photon emission dynamics from two single QDs in a high quality PPC nanocavity; we also compute the quantum emission (first-order quantum correlation function) and the entanglement of formation between the two excitonic qubits. The work is fully quantum in nature, and no classical field is assumed. Further, we account for different QD parameters, such as dipole moments and transition energies, and find original entanglement situations that have no counterpart with identical atoms.

The photon Green function is a key material property that can be exploited in quantum optics since it relates directly to how photons propagate. In fact, the excitement that PCs bring to the scientific playground is driven by their ability to modify the GFT properties in a profound way. For example, periodic patterning of the composite dielectric material can result in photonic band gaps (PBGs), where light propagation is not allowed at all; these characteristics can also strongly modify the SE of excited QDs that are placed within the PC. The underlying physics of such phenomena can be elegantly described by analyzing the appropriate GFTs; e.g., the GFT can be used to obtain an integral solution to both the macroscopic and microscopic Maxwell equations [10,11] and can also be used on its own for obtaining the SE rate. In the weak-coupling regime, the enhanced SE factor is correctly termed the Purcell factor [12].

While the current analysis of optical properties in PCs is frequently carried out using large scale numerical techniques, the idea of connecting the underlying optical processes to the GFT is certainly not new. Indeed, as pointed out by Lodahl *et al.* [3], controlling the dynamics of SE from *weakly coupled* QDs in PCs can be intuitively understood by making a connection to the photon local density of states (LDOS), which is simply related to the GFT through $\mathrm{LDOS}(\mathbf{r}) \propto \mathrm{Trace}\{\Im[\vec{\mathbf{G}}(\mathbf{r}, \mathbf{r}; \omega)]\}$. From a quantum optics perspective, one is interested in exploiting a large LDOS that can be realized over a relatively small frequency range; this can be used, e.g., to create an efficient single photon emitter. Interestingly, this desired feature is entirely natural to PPCs since they can exhibit a large PBG (and thus negligibly small LDOS or vacuum fluctuations), and the sudden increase in the LDOS is realized by creating defects. Since a PPC is typically made up of a regular lattice of air holes, defects are simply created by the controlled omission of air holes in a high-index semiconductor. One such structure is shown in Fig. 1 that depicts a defect nanocavity containing two QDs. This is the structure of interest for our study, and is similar to experimental samples in which single QD strong coupling was recently observed [4]. The one QD strong coupling quantum dynamics is described elsewhere [13].

The quantized electric field can be expressed as $\hat{\mathbf{E}}(\mathbf{r}) = \int d\mathbf{r}' \vec{\mathbf{G}}^b(\mathbf{r}, \mathbf{r}'; \omega) \cdot \hat{\mathbf{P}}(\mathbf{r}')/\epsilon_0$, where $\hat{\mathbf{P}}$ is the polarization operator and $\vec{\mathbf{G}}^b$ is the ideal GFT of the background nanocavity obtained from $[\nabla \times \nabla \times + (\omega/c)^2 \epsilon_c(\mathbf{r})] \times \vec{\mathbf{G}}^b(\mathbf{r}, \mathbf{r}'; \omega) = (\omega/c)^2 \vec{\mathbf{1}} \delta(\mathbf{r} - \mathbf{r}')$, with $\vec{\mathbf{1}}$ the unit tensor and ϵ_c the permittivity of the nanocavity structure. The defined GFT is for the complete solution of the full Maxwell equations, and we keep the factor $(\omega/c)^2$ on the right-hand side since the GFT can then also be obtained numerically for any shaped nanostructure (see, e.g., Hughes *et al.* [14]). The relevant GFT can then be written as $\vec{\mathbf{G}}^b(\mathbf{r}, \mathbf{r}'; \omega) = \vec{\mathbf{G}}^t(\mathbf{r}, \mathbf{r}'; \omega) - \delta(\mathbf{r} - \mathbf{r}')\vec{\mathbf{1}}/|\epsilon_c(\mathbf{r})|$, where the former contribution only contains quasitransverse modes of the cavity and the latter (purely real) contribution also contains the quasilongitudinal modes and will play no role in what follows. We also define the fundamental cavity mode normalized from the $\mathbf{E}$ field of the cavity as $\mathbf{e}_c = \boldsymbol{\phi}_c/\sqrt{V_m}$, with $|\boldsymbol{\phi}_c|^2 = |\mathbf{E}_c|^2/\max[\epsilon_c|\mathbf{E}_c|^2]$, where the effective mode volume $V_m = \int_{\text{all space}} d\mathbf{r} \epsilon_c(\mathbf{r})|\boldsymbol{\phi}_c(\mathbf{r})|^2$. The important cavity contribution can then be obtained from $\vec{\mathbf{G}}^t(\mathbf{r}, \mathbf{r}'; \omega) = \omega_c^2 \mathbf{e}_c(\mathbf{r}) \otimes \mathbf{e}_c^*(\mathbf{r}')/[\omega_c^2 - \omega^2 - i\omega\Gamma_c]$, where ω_c is the cavity resonance frequency and $\Gamma_c = \omega_c/Q$ is the cavity linewidth rate. Although the above GFT contains only one resonance, it is actually quite typical of a semiconductor PC defect mode that exists deep in the PBG, and a small finite coupling to radiation modes is contained within the cavity linewidth rate; we have also verified this numerically using a direct solution of the Maxwell equations. The boundary conditions on the GFT is such that is includes the entire nanocavity and its surrounding.

We consider the decay dynamics from two coupled QDs that have the states a and b as their respective *upper excited level*. We also assume QDs that have a well defined fundamental exciton transition, with a diameter much smaller than the wavelength of light. The initial field is assumed in vacuum so all the ensuing dynamics will be driven by the initially excited QD(s). Working within a framework for quantizing the macroscopic electromagnetic fields in arbitrary dispersing and absorbing surroundings, and exploiting a general interaction (multipolar) Hamiltonian that employs the dipole and rotating wave approximation, one can derive the upper-level decays as [15]

$$\dot{C}_a(t) = \int_0^t dt' [\mathcal{A}_{r_a r_a}(t, t') C_a(t') + \mathcal{A}_{r_a r_b}(t, t') C_b(t')] \tag{1}$$

$$\dot{C}_b(t) = \int_0^t dt' [\mathcal{A}_{r_b r_b}(t, t') C_b(t') + \mathcal{A}_{r_b r_a}(t, t') C_a(t')], \tag{2}$$

where $\mathcal{A}_{r_\alpha r_\beta}(t, t') = -1/(\hbar\pi\epsilon_0) \int_0^\infty d\omega e^{-i(\omega-\omega_\alpha)t} \times e^{i(\omega-\omega_\beta)t'} \mathbf{d}_\alpha^* \cdot \Im[\vec{\mathbf{G}}^b(r_\alpha, r_\beta; \omega)] \cdot \mathbf{d}_\beta$, $(\alpha, \beta = a, \text{or } b)$ with ω_i and $\mathbf{d}$ the resonance frequency and dipole moment of the QD. Additionally, the first-order quantum correlation function $\langle \mathbf{E}^+(\mathbf{r}, t) \cdot \mathbf{E}^-(\mathbf{r}, t) \rangle \propto |\Sigma_{\alpha=a,b}[\int_0^t dt' \times \int_0^\infty d\omega C_\alpha(t') \Im[\vec{\mathbf{G}}^b(\mathbf{r}, r_\alpha; \omega)] \cdot \mathbf{d}_\alpha e^{-i(\omega-\omega_\alpha)(t-t')}]|^2$, where the additional GFT is required to describe photon propagation from the QD to the point detector at position $\mathbf{r}$.

Next we wish to make a connection to the degree of entanglement that can achieved. Entanglement is a well established quantum property that has no counterpart in classical optics, and occurs when the total wave function of the mixed system cannot be written in any basis, as a direct product of independent substates. Since we find that the 1 QD strong coupling scenario can be equally described classically or quantum mechanically [9] (indeed this is well known), we need at least two QDs here to make a connection to exploring any entanglement effects due to qubit-qubit correlations. Here the entanglement (E) is cal-

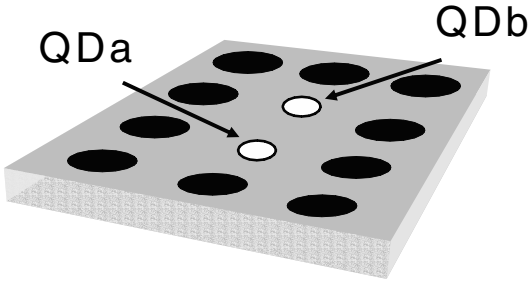

FIG. 1. Simple schematic of a semiconductor PPC nanocavity. The holes represent etched air holes, and a deliberate missing hole forms a defect nanocavity; two quantum dots (QDs) are embedded near a field antinode that contains one electron-hole pair in the spectral region of interest. In reality, of course, the PPC contains many more holes.

culated from the concurrence $[C(t)]$ [16] through $E(t) = -x\log_2(x) - (1-x)\log_2(1-x)$ $[x = 0.5 + 0.5\sqrt{1 - C(t)}]$. For this we need the reduced density matrix of our 2-qubit system $\rho_{ab}(t) = |\psi(t)\rangle\langle\psi(t)|$, where the elements of the wave function $|\psi\rangle$ are obtained from Eqs. (1) and (2). Lastly, we introduce a quantum mechanical basis for the QDs a and b, and the photon field (cavity) as $|A\rangle \otimes |B\rangle \otimes |k\rangle = |ABk\rangle$, where each state can take a value of 0 or 1. Tracing out the cavity field, we employ the following initial condition for the two QD system: $|\psi(t=0)\rangle = \cos(\theta)|10\rangle + e^{i\phi}\sin(\theta)|01\rangle$, that can be prepared through appropriate (and careful) optical excitation of the solid-state QD system.

Let us summarize the basic theoretical approach and highlight its range of validity. Assuming that one knows the GFT response of the surrounding environment, the propagation of photons from the dipolelike QDs and the 1-exciton QD quantum dynamics can be accounted for semiquantitatively by the above equations. Moreover, for a typical PPC nanocavity that contains a resonance deep inside the PBG, the GFT used above is also an excellent approximation. Consequently, one can proceed to investigate the complex coupling dynamics of many single QDs within such a system and expect to gain an accurate and intuitive understanding of the underlying physics. Outside some of the basic approximations that we make, we are not aware of any other methods for solving this highly complex semiconductor problem, while keeping things general enough to include the essential effects such as dispersion (and absorption) in the medium, different QD parameters, and different positions within the cavity.

For the calculations we adopt *nominal* parameters representative of realistic semiconductor PPC nanocavities, with $Q = 15000$ (corresponding $\Gamma_c \approx 0.06$ meV), $\omega_c/(2\pi) = 230$ THz, and cavity mode volume $V_m = 0.05\ \mu\text{m}^3$. We note that although experimental cavity Qs in PPC nanocavities now surpasses 45 000 [6], we choose to use conservative Q values to account for the fact that the QDs may not be on the peak antinode of the field. For the QD we employ similar parameters from single QD optical experiments with *nominal* dipole moment $d = d_0 = 60$ D [17] and ω_α close to the cavity resonance. Below, we investigate several *Gedanken* experiments that are fully motivated by related measurements that are currently being actively investigated within the scientific community.

First we consider the SE and entanglement dynamics associated with dot a initially excited, and with dot b in the ground state, at time $t = 0$. Thus the initial wave function $|\psi(t=0)\rangle = |10\rangle$. For now, we assume that both QDs are on resonance with the cavity and that the QDs have equivalent positions within the PPC cavity [$\mathcal{A}_{r_a r_a} = \mathcal{A}_{r_b r_b} = \mathcal{A}_{r_a r_b} = \mathcal{A}_{r_b r_a}$ in Eqs. (1) and (2)]. Such a situation is commonly investigated for atomic systems and can be realized here when the QDs are in close proximity and lying at either side of the cavity [7]. In Fig. 2(a) we show the ensuing emission dynamics of QD a (solid curve), b (dashed curve), and the entanglement E (chain curve). These results show that, for these initial conditions, $E = 0.35$ ebits (corresponding to a concurrence of 0.5) is the maximum amount possible, which is identical to the perfect atomic case. For comparison, we also calculate E when the QDs are at different equivalent locations in the cavity ($|\mathbf{E}_c(r_b)|^2 = |0.9\mathbf{E}_c(r_a)|^2$), yielding more complex behavior (dotted curve) though the general picture remains unchanged.

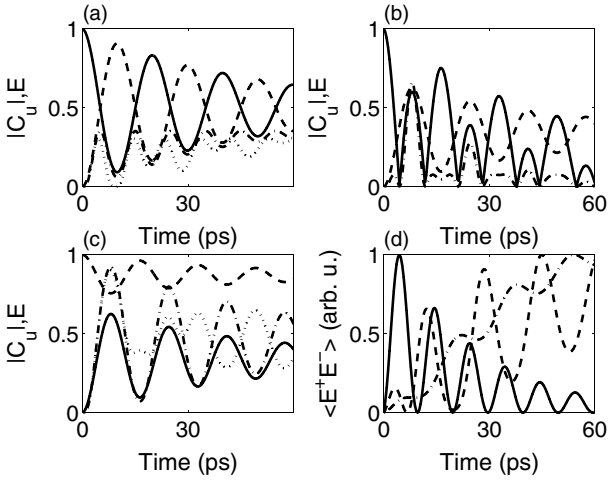

FIG. 2. (a) Upper decay of the quantum dots a (solid curve) and b (dashed curve), and the entanglement (chain curve); the dotted curve shows E with slightly different QD positions in the cavity (see text). (b) As in (a) but with $d_a = 1.6d_b$. (c) As in (b) but with QD b initially excited; the dotted curve shows E with 0.1 meV detuning between the QDs. (d) Corresponding first-order quantum correlation function for nominal cases in Fig. 2(a)–2(c) shown, respectively, by the solid, dashed, and chain curve.

We now look at QDs with different dipole moments, namely $d_a = 1.6d_0$ and $d_a d_b = d_0^2$ (equivalent dipole-dipole-coupling strength). In Fig. 2(b) are shown the results with an identical initial condition to above that, that although displays a larger E near 10 ps (≈ 0.6), yields a much smaller value than 0.35 for longer times. In contrast, as shown in Fig. 2(c), we find that when QD b is initially excited ($|\psi(t=0)\rangle = |01\rangle$), rather than QD a, then E becomes considerably more than 0.35 at both early and long times. This is obviously advantageous over an identical pair of atoms for creating entangled pairs from a one QD excited initial condition, since the dipole asymmetry allows one to probe quite different E dynamics than the equal dipole case; the level populations now oscillate around different values, and such a situation offers significantly greater flexibility than an identical atom system. In addition, we also calculate E when QD b is detuned by 0.1 meV from the cavity (dotted curve), and numerically confirm that such large E values are also possible when d_0 is decreased by a factor of 3–4 (the first large peak then appears at a greater time of around 30 ps). The corresponding emission $\langle \mathbf{E}^+(\mathbf{r}, t) \cdot \mathbf{E}^-(\mathbf{r}, t)\rangle$ is also calculated and

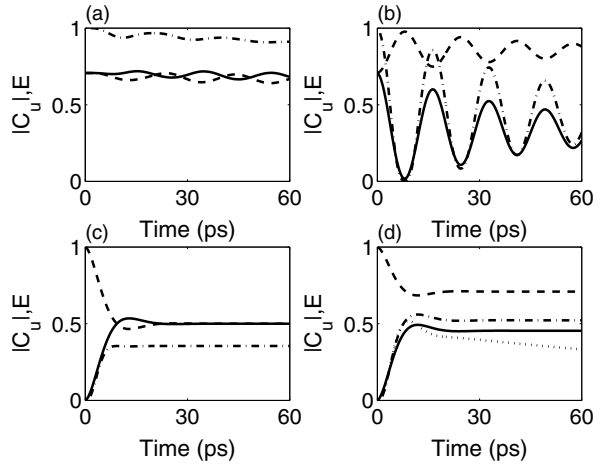

FIG. 3. (a) Upper decay of the entangled quantum dots a (solid curve) and b (dashed curve), and the entanglement E (chain curve); the QDs are detuned by 0.1 meV. (b) As in (a) but with $d_a = 1.6d_b$ and no detuning between the dots. (c) Equal dipole moment QDs in a reduced Q cavity (factor of 10 smaller than the above). (d) As in (c) but with $d_a = 1.3d_b$; the dotted curve shows E with 0.1 meV detuning between the QDs.

displayed in Fig. 2(d) for the three nominal cases in Fig. 2(a)–2(c), showing SE dynamics that are substantially different. However, common to all, pronounced strong coupling and photon exchange effects are clearly observed, as is the onset of nontrivial quantum dynamics due to different optical dipole moments.

Next we investigate an initially *maximally entangled 2-qubit state*, with $|\psi(t=0)\rangle = 2^{-1/2}[|10\rangle \pm |01\rangle]$. The in-phase ("+") solution results in qubit entanglement that falls off slightly faster than in the previous cases, while the out-phase ("−") solution can result in perfect entanglement and no photons will be detected. Thus, for proper excitation of the two QD system, no decay takes place from the QD excitons, and zero is obtained for the quantum correlation function. This rather profound result can be traced back to the fact that we prepare an ideal superposition eigenstate of the mixed system, namely $|U_\pm\rangle = 2^{-1/2}[|a\rangle \pm |b\rangle]$, whose decay depends only on the sum or difference of the self-QD and cross-QD coupled GFT elements. To consider the robustness of this remarkable situation we calculate the quantum dynamics with different dipole moments and transition energies between the two QDs. In Fig. 3(a) is shown the dot dynamics and E when QD b is detuned by 0.1 meV, displaying only a minor effect on the longer time dynamics. Thus the scheme is fairly robust with respect to small detunings between the QDs (E *is still greater than 0.9 after 60 ps*). In Fig. 2(b) we also set $d_a = 1.6d_0$ again, yielding E dynamics that oscillate significantly—clearly picking up the strong coupling regime for both QDs; the longer time behavior is now similar to that obtained in Fig. 2(a).

It is also known for perfect atomic systems that $E > 0.35$ can never be achieved when one QD is initially excited and the other is in the ground state [18]. To come close to this situation, we reduce the Q of the cavity by a factor of 10 ($Q = 1500$), and initially set the QD dipole moments equal. In Fig. 3(c) we recover the situation that the E indeed approaches 0.35 ebits. However, when we change the dipole moments to $d_a = 1.3d_0$ [19] [see Fig. 3(d)], then the dipole asymmetry in the system again allows much higher E to be achieved, resulting in values greater than 0.35 (chain curve); lastly, we also present calculations with 0.1 meV detuning between the QDs (dotted curve) that yield a slight decay of these values.

To conclude, we have introduced a scheme that allows one to study quantum correlations between two single QDs dots within in a PPC nanocavity. A powerful self-consistent GFT approach is described that captures the dominant quantum optical phenomena, yet the theory is remarkably intuitive and covers all coupling regimes in a straightforward manner. We subsequently predict SE dynamics that are much richer than for simple atomic systems and lead to sizable amounts of qubit entanglement for many cases—a highly desired property for quantum information science.

The author thanks D. S. Citrin, L. Ramunno, and H. Kamada for stimulating discussions.

*Address from July 2005: Department of Physics, Queen's University, Kingston, Ontario, Canada K7L 3N6.

[1] E. Yablonovitch, Phys. Rev. Lett. **58**, 2059 (1987).
[2] S. John, Phys. Rev. Lett. **58**, 2486 (1987).
[3] P. Lodahl *et al.*, Nature (London) **430**, 654 (2004).
[4] T. Yoshie *et al.*, Nature (London) **432**, 200 (2004).
[5] For a textbook discussion, see, for example, P. Meystre and M. Sargent III, *Elements of Quantum Optics* (Springer, New York, 1997), 3rd ed..
[6] Y. Akahane *et al.*, Nature (London) **425**, 944 (2003).
[7] E. Hagley and S. Haroche *et al.*, Phys. Rev. Lett. **79**, 1 (1997).
[8] For a textbook discussion, see, for example, M. O. Scully and M. S. Zubairy, *Quantum Optics* (Cambridge University Press, Cambridge, England, 1997).
[9] S. Hughes and H. Kamada, Phys. Rev. B **70**, 195313 (2004).
[10] See, for example, B. Huttner and S. M. Burnett, Phys. Rev. A **46**, 4306 (1992).
[11] See, for example, Y. Xu *et al.*, Phys. Rev. A **61**, 033807 (2000).
[12] E. M. Purcell, Phys. Rev. **69**, 37 (1946).
[13] S. Hughes, Opt. Lett. **30**, 1393 (2005).
[14] S. Hughes *et al.*, Phys. Rev. Lett. **94**, 033903 (2005).
[15] H. T. Dung, L. Knöll, and D.-G. Welsch, Phys. Rev. A **66**, 063810 (2002).
[16] W. K. Wootters, Phys. Rev. Lett. **80**, 2245 (1998).
[17] H. Kamada *et al.*, Phys. Rev. Lett. **87**, 246401 (2001).
[18] H. T. Dung *et al.*, J. Opt. B **4**, S169 (2002).
[19] Note that 1.3 works better than 1.6 in this case—though we have not fully optimized this situation.